Low-complexity joint data detection and channel equalisation for highly mobile orthogonal frequency division multiplexing systems

H. Doğan[1]   E. Panayırcı[2],*   H. Vincent Poor[2]

[1]Department of Electrical and Electronics Engineering, Istanbul University, Avcilar, Istanbul 34320, Turkey
[2]Department of Electrical Engineering, Princeton University, Princeton NJ 08544, USA
*On sabbatical leave from Kadir Has University, Istanbul, Turkey
E-mail: hdogan@istanbul.edu.tr

Abstract: This study is concerned with the challenging and timely problem of channel equalisation and data detection for orthogonal frequency division multiplexing (OFDM) systems in the presence of frequency-selective and very rapidly time-varying channels. The algorithm is based on the space alternating generalised expectation-maximisation (SAGE) technique which is particularly well suited to multicarrier signal formats and can be easily extended to multi-input multi-output-OFDM systems. In fast fading channels, the orthogonality between subcarriers is destroyed by the time variation of a fading channel over an OFDM symbol duration which causes severe inter-carrier interference (ICI) and, in conventional frequency-domain approaches, results in an irreducible error floor. The proposed joint data detection and equalisation algorithm updates the data sequences in series leading to a receiver structure that also incorporates ICI cancellation, enabling the system to operate at high vehicle speeds. A computational complexity investigation as well as detailed computer simulations indicate that this algorithm has significant performance and complexity advantages over existing suboptimal detection and equalisation algorithms proposed earlier in the literature.

1   Introduction

Orthogonal frequency division multiplexing (OFDM) has been shown to be an effective method to overcome inter-symbol interference (ISI) effects because of frequency-selective fading with a simple transceiver structure, and as a consequence is used in several existing wireless local and metropolitan area standards such as the IEEE 802.11 and IEEE 802.16 families. IEEE 802.11 wireless local area networks are very useful for providing different data services to Internet users, but their overall design and feature set are not well suited for outdoor broadband wireless access (BWA) applications [1]. Therefore IEEE 802.16 has been developed as a new standard for BWA applications [2]. Recently, long-term evolution (LTE) and worldwide interoperability for microwave access (WiMAX)

technologies have become the latest steps towards the fourth generation of radio technologies designed to enable mobile broadband services at vehicular speeds beyond 100 km/h. They will potentially allow data transfer rates to and from mobile devices between 15 and 100 times faster than 3G networks.

OFDM eliminates ISI and simply uses a one-tap equaliser to compensate for multiplicative channel distortion in quasi-static channels. However, in fading terminals with very high mobility, the time variations of the fading channel over an OFDM symbol period can result in a loss of subchannel orthogonality, which in turn leads to inter-carrier interference (ICI). A considerable amount of research has been devoted to the development of OFDM receivers based on a quasi-static fading model, while the

major hindrance is the lack of mobility support [3–5]. Since mobility support is widely considered to be one of the key features in wireless communication systems and in this case ICI degrades the performance of OFDM systems, a major challenge is the development of techniques for OFDM transmission over very rapidly time-varying multipath fading channels.

One study of this problem is [6], in which the performance of the matched filter (MF), linear least squares (LS), linear minimum mean square error (MMSE) and MMSE with successive detection (SD) techniques were investigated. It was shown that the MMSE detection technique is able to exploit the time-varying channel as a source of time diversity while it still results in residual interference, causing performance degradation for higher order modulation. Thus, in order to effectively mitigate both interference and noise, MMSE with SD, known as VBLAST (Vertical-Bell Laboratories Layered Space–Time), was proposed in [6] to achieve time diversity for higher order modulation. However, the complexity requirements for this detection process were not considered in [6].

Applications of the space-alternating generalised expectation-maximisation (SAGE) algorithm, a modified version of the expectation maximisation (EM) technique have been considered for several aspects of receiver design for wireless communication systems. The principal approaches to apply these techniques to multiuser detection are surveyed in [7]. For code-division multiple-access (CDMA) systems, the work [8] extended the EM and SAGE algorithms for detection of multiuser signals, and later these iterative techniques were investigated in [9] for multiuser detection in multipath CDMA channels with iterative space–time processing. In [10], iterative receivers are derived for joint channel estimation and detection in direct-sequence (DS)-CDMA to avoid multiple access interference. Recently, EM and SAGE algorithms have been applied to maximum likelihood (ML) channel estimation for uplink DS-CDMA systems operating over time-varying fading channels [11]. It was shown that both algorithms achieve the benefits of the ML estimator when direct computation of the matrix inversion required for ML estimation is too complex. It was further demonstrated that the SAGE algorithm yields faster convergence than the EM algorithm.

In this paper, a computationally feasible SAGE algorithm is proposed for the problem of joint data detection and channel equalisation for OFDM systems operating in highly mobile and frequency-selective channels [11, 12]. The channel variation over the duration of a data block is upper bounded by the maximum Doppler bandwidth which is determined by the maximum speed of the users. It is seen that the resulting SAGE-based receiver scheme comprises ICI cancellation and a soft-input/hard-output serial data detector in each iteration. The proposed algorithm is compared with previously studied algorithms

in terms of both symbol error rate (SER) and complexity requirements. The tradeoff between complexity and SER performance is investigated. It is shown through simulation that the performance degradation caused by ICI can be compensated effectively by the proposed low-complexity receiver.

The paper is organised as follows. Section 2 presents the observation signal model for highly mobile OFDM systems and describes the time-varying channel model. In Section 3, some equalisation and detection techniques are reviewed. In Section 4, the proposed SAGE algorithm is presented for joint data detection and channel equalisation. Furthermore, we present a low-complexity initialisation algorithm and discuss the computational complexity issues. In Section 5, the performance of the proposed algorithm is evaluated via computer simulations. Finally, Section 6 summarises the main conclusions of the paper.

2　System model

Let us consider an OFDM system with N subcarriers and available bandwidth $B = 1/T_s$, where T_s is the sampling period. The available bandwidth is divided into N subchannels by equal frequency spacing $\Delta f = B/N$. At the transmitter, information bits are mapped into possibly complex-valued transmitted symbols according to the modulation format employed. The symbols are processed by an N-length inverse fast Fourier transform block that transforms the data symbol sequence into the time domain. The time-domain signal is extended by a guard interval containing G samples whose length is chosen to be longer than the expected delay spread to avoid ISI. The guard interval includes a cyclically extended part of the OFDM symbol to avoid ISI. Hence, the complete OFDM block duration is $P = N + G$ samples. The resulting signal is converted to an analogue signal by a digital-to-analogue (D/A) converter. After shaping with a low-pass filter (e.g. a raised-cosine filter) with bandwidth B, it is transmitted through the transmit antenna with the overall symbol duration of $T = PT_s$.

Let $h(m, l)$ represent the lth path (multipath component) of the time-varying channel impulse response at time instant $t = mT_s$. The discrete-time received signal can then be expressed as follows

$$y(m) = \sum_{l=0}^{L-1} h(m, l) d(m - l) + w(m) \qquad (1)$$

where the transmitted signal $d(m)$ at discrete sampling time m is given by

$$d(m) = \frac{1}{\sqrt{N}} \sum_{k=0}^{N-1} s(k) e^{j2\pi mk/N} \qquad (2)$$

L is the total number of paths of the frequency-selective fading channel, and $w(m)$ is the additive white Gaussian

noise with zero mean and variance $E\{|w(m)|^2\} = \sigma_w^2$. The sequence $s(k)$, $k = 0, 1, \ldots, N - 1$, in (2) represents either quadrature-amplitude modulation (QAM) or phase-shift-keying (PSK) modulated data symbols.

At the receiver, after passing through the analogue-to-digital (A/D) converter and removing the cyclic prefix (CP), a fast Fourier transform (FFT) is used to transform the data back into the frequency domain. Lastly, the binary data are obtained after demodulation and channel decoding.

The fading channel coefficients $h(m, l)$ can be modelled as zero-mean complex Gaussian random variables. Based on the wide-sense stationary uncorrelated scattering assumption, the fading channel coefficients in different paths are uncorrelated with each other. However, these coefficients are correlated within each individual path and have a Jakes Doppler power spectral density [13] having an autocorrelation function given by

$$E\{h(m, l)h^*(n, l)\} = \sigma_{h_l}^2 J_0(2\pi f_d T_s(m - n)) \quad (3)$$

where $\sigma_{h_l}^2$ denotes the power of the channel coefficients of the lth path. f_d is the Doppler frequency in Hertz and $J_0(\cdot)$ is the zeroth-order Bessel function of the first kind.

By substituting (2) into (1), the received signal can be written as

$$y(m) = \frac{1}{\sqrt{N}} \sum_{k=0}^{N-1} s(k) \sum_{l=0}^{L-1} h(m, l) e^{j2\pi k(m-l)/N} + w(m) \quad (4)$$

which upon defining the time-varying channel transfer function $H(k, m) \triangleq \sum_{l=0}^{L-1} h(m, l) e^{-j2\pi lk/N}$ becomes

$$y(m) = \frac{1}{\sqrt{N}} \sum_{k=0}^{N-1} s(k) H(k, m) e^{j2\pi mk/N} + w(m) \quad (5)$$

The FFT output at the kth subcarrier can be expressed as

$$Y(k) = \frac{1}{\sqrt{N}} \sum_{m=0}^{N-1} y(m) e^{-j2\pi mk/N}$$

$$= s(k)H(k) + I(k) + W(k) \quad (6)$$

where $H(k)$ represents the average frequency-domain channel response, defined as

$$H(k) \triangleq \frac{1}{N} \sum_{m=0}^{N-1} H(k, m) \quad (7)$$

$I(k)$ is the ICI caused by the time-varying nature of the channel given as

$$I(k) = \frac{1}{N} \sum_{i=0, i \neq k}^{N-1} s(i) \sum_{m=0}^{N-1} H(i, m) e^{j2\pi m(i-k)/N} \quad (8)$$

and $W(k)$ denotes the discrete Fourier transform of the white Gaussian noise $w(m)$

$$W(k) = \frac{1}{\sqrt{N}} \sum_{m=0}^{N-1} w(m) e^{-j2\pi mk/N} \quad (9)$$

When the channel is quasi-static or slowly time varying then $H(i, m) \simeq H(i)$ and $I(k) = 0$ since the second summation in (8) becomes zero. Consequently, it can be easily shown from (6) that the received signal at the output of FFT takes the known form

$$Y(k) = s(k)H(k) + W(k), \quad k = 0, 1, \ldots, K - 1$$

Note that because of the term $I(k)$ in (6), there is an irreducible error floor even in the training sequences since pilot symbols are also corrupted by ICI, arising from the fact that the time-varying channel destroys the orthogonality between subcarriers.

The received signal after FFT processing can be expressed in the frequency domain in vector form as

$$Y = Hs + W \quad (10)$$

where $Y = [Y(0), Y(1), \ldots, Y(N - 1)]^T$, $s = [s(0), s(1), \ldots, s(N - 1)]^T$, $W = [W(0), W(1), \ldots, W(N - 1)]^T$. The time-varying channel matrix H is defined from (7) and (8) as follows

$$H[k, i]$$

$$= \begin{cases} H(k) & \text{if } i = k \\ (1/N) \sum_{m=0}^{N-1} H(i, m) \exp(j2\pi m(i - k)/N) & \text{if } i \neq k \end{cases}$$

$$(11)$$

where the first and second indices of $H[\cdot, \cdot]$ in (11) represent the discrete frequency and time variables, respectively.

3 Review of some detection techniques for OFDM systems

Under the assumption that the channel matrix H in (11) is perfectly known at the receiver, the ML detector performs an exhaustive search over the entire set of signal vectors whose components are selected from the signal constellation formed by the modulation scheme chosen. Especially in WiMAX and LTE-based OFDM systems, the length N of each OFDM symbol is very large; it can take values as large as $N = 1024$, especially for high mobility applications. In this case an exhaustive search for the ML solution would be very complex since the search space has an extremely large number of constellation points ($|\mathcal{S}|^N$, where $|\mathcal{S}|$ is the cardinality of the signal constellation). Therefore it is necessary to consider

Table 1 Linear detection methods

Method	Solution
matched filter	$\hat{\boldsymbol{s}} = Q\{\boldsymbol{H}^{\dagger}\boldsymbol{Y}\}$
zero forcing	$\hat{\boldsymbol{s}} = Q\{(\boldsymbol{H}^{\dagger}\boldsymbol{H})^{-1}\boldsymbol{H}^{\dagger}\boldsymbol{Y}\}$
MMSE	$\hat{\boldsymbol{s}} = Q\{(\boldsymbol{H}^{\dagger}\boldsymbol{H} + \sigma_w^2\boldsymbol{I})^{-1}\boldsymbol{H}^{\dagger}\boldsymbol{Y}\}$

suboptimal solutions having much lower computational complexity.

In linear equalisation-based detection techniques, an estimate of the transmitted data vector $\boldsymbol{s}$ is formed as $\hat{\boldsymbol{s}} = \boldsymbol{G}^{\dagger}\boldsymbol{Y}$ with an 'equalisation matrix' $\boldsymbol{G}^{\dagger}$. Given the channel matrix $\boldsymbol{H}$, linear methods for detecting $\boldsymbol{s}$ are listed Table 1 where $Q(\cdot)$ denotes component-wise quantisation according to the symbol alphabet of the modulation technique. The conventional matched-filter detector, which neglects the presence of ICI, is the simplest linear detector. Therefore its performance is limited because the orthogonality of the subcarriers does not hold in a time-varying channel. To reduce ICI effects, the zero-forcing (ZF) equaliser $\boldsymbol{G}^{\dagger}$ given by the pseudo-inverse as shown in Table 1 can be applied. However, the ZF equaliser amplifies the noise at frequencies where the channel response $\boldsymbol{H}$ has a small magnitude (near zeroes of the channel) in order to invert the channel completely. In other words, in the ZF equaliser, the transformed noise, $\tilde{\boldsymbol{W}} = \{(\boldsymbol{H}^{\dagger}\boldsymbol{H})^{-1}\boldsymbol{H}^{\dagger}\boldsymbol{W}\}$, can have much larger variance than $\boldsymbol{W}$ (noise enhancement). The noise enhancement effect of the ZF equaliser can be reduced by using the MMSE equalizer in which $\boldsymbol{G}^{\dagger}$ is chosen to minimise the mean-square error $E\{\|\boldsymbol{G}^{\dagger}\boldsymbol{y} - \boldsymbol{s}\|^2\}$. The MMSE equaliser

mitigates both the residual interference and the noise enhancement. It becomes the ZF solution when no noise is present. However, the residual interference and the noise enhancement grow as the normalised Doppler frequency becomes large, and hence the MMSE equaliser performance is also limited under these conditions. This effect can be seen significantly for higher order modulation and SNR values. On the other hand, all of the linear equalisers given in Table 1 are suboptimal since they do not take into account the correlation of the components of the transformed noise.

It has been shown that the time-varying nature of the mobile channel can be exploited as a provider of time diversity when the normalised Doppler frequency becomes large. In [6], to fully exploit the time diversity while suppressing the residual interference and the noise enhancement, a recursive detection technique using the decision-feedback principle, namely the MMSE-SD algorithm (VBLAST), has been proposed. In this algorithm, at each detection step, a single data vector component is detected and the corresponding contribution to the received vector $\boldsymbol{Y}$ is subtracted from $\boldsymbol{Y}$. In other words, the data symbols are detected one-by-one instead of simultaneously. The detailed detection procedure of the VBLAST algorithm is given in Table 2 where $\boldsymbol{g}_k$ is the kth column vector of the equaliser matrix $\boldsymbol{G}$. The performance of VBLAST depends critically on the order in which the data vector components are processed. To minimise error propagation effects and to improve the detection of unreliable components, more reliable data vector components should be detected first. Therefore the algorithm depends on calculation of the post-detection signal-to-interference plus noise ratio (SINR) based upon

Table 2 MMSE with successive detection (SD)

$j = 1$
$\boldsymbol{G}^{\dagger} = (\boldsymbol{H}^{\dagger}\boldsymbol{H} + \sigma_w^2\boldsymbol{I}_N)^{-1}\boldsymbol{H}^{\dagger}$
$i_I = \arg\max\limits_{k}\left\{\text{SINR}_k = \dfrac{|\langle\boldsymbol{g}_k, \boldsymbol{h}_k\rangle|^2}{\sum_{m=1,m\neq k}|\langle\boldsymbol{g}_k, \boldsymbol{h}_k\rangle|^2 + \sigma_w^2\|\boldsymbol{g}_k\|^2}\right\}$
loop
$s_{i_{(j)}} = \boldsymbol{g}_{i_{(j)}}^{\dagger}\boldsymbol{Y}$
$\hat{s}_{i_{(j)}} = Q\{s_{i_{(j)}}\}$
$\boldsymbol{Y} = \boldsymbol{Y} - \boldsymbol{h}_{i_{(j)}}\hat{s}_{i_{(j)}}$
$\boldsymbol{H} = [\boldsymbol{h}_0 \cdots \boldsymbol{h}_{i_{(j-1)}} \quad 0 \quad \boldsymbol{h}_{i_{(j+1)}} \cdots \boldsymbol{h}_{N-1}]$
$\boldsymbol{G}^{\dagger} = (\boldsymbol{H}^{\dagger}\boldsymbol{H} + \sigma_w^2\boldsymbol{I}_N)^{-1}\boldsymbol{H}^{\dagger}$
$i_{(j+1)} = \arg\max\limits_{k\in\{i_1,\ldots,i_j\}}\left\{\text{SINR}_k = \dfrac{|\langle\boldsymbol{g}_k, \boldsymbol{h}_k\rangle|^2}{\sum_{m=1,m\in\{i_1,\ldots,i_j\},m\neq k}|\langle\boldsymbol{g}_k, \boldsymbol{h}_k\rangle|^2 + \sigma_w^2\|\boldsymbol{g}_k\|^2}\right\}$
$j = j + 1$

MMSE detection as a measure of reliability. Calculation of the SINR is compulsory at each iteration, and therefore this algorithm is computationally intensive as a number of pseudo-inverse operations need to be performed. Moreover, its complexity grows exponentially with the total number of subcarriers. Therefore, in the next section, we propose a new SAGE based detection algorithm in which there is no need to calculate the SINR at each iteration.

4 Signal detection with the SAGE algorithm

The SAGE algorithm, first introduced by Fessler and Hero [14], is a generalisation of the classical EM algorithm. It has been shown to be particularly suitable for estimation of superimposed signals in Gaussian noise and to be much faster than the EM algorithm. EM and SAGE algorithms have been applied to channel estimation in DS-CDMA and OFDM systems where the parameter set is continuous. However, for data detection, in which the parameter set is discrete, the problem is different from that of channel estimation. In this paper, we apply the SAGE algorithm for the detection of OFDM signals over fast fading channels [12] and thus must consider this issue.

Basically, the EM algorithm provides an iterative scheme by updating all parameters simultaneously at each iteration; under appropriate conditions its performance approaches that of ML as the number of iterations increases. On the other hand, in the SAGE algorithm only a subset of the parameters to be estimated is updated while the parameters in the complement set are held fixed. Also, the concept of incomplete data employed in the EM algorithm is extended to that of the so-called hidden data to which the incomplete data are related by means of a possibly non-deterministic mapping having properties to guarantee that the SAGE algorithm exhibits the monotonicity property of the EM scheme.

The symbol detection architecture considered in this paper can be derived within the SAGE framework as follows: The received vector $\boldsymbol{Y}$ is decomposed in terms of the column vectors of $\boldsymbol{H}$, defined in (11), as

$$\boldsymbol{Y} = \boldsymbol{h}_0 s(0) + \boldsymbol{h}_1 s(1) + \cdots + \boldsymbol{h}_{N-1} s(N-1) + \boldsymbol{W} \quad (12)$$

where $\boldsymbol{h}_n = [\boldsymbol{H}[n, 0], \boldsymbol{H}[n, 1], \dots, \boldsymbol{H}[n, N-1]]^{\mathrm{T}}$.

The parameter vector to be estimated is $\boldsymbol{s} = [s(0), s(1), \dots, s(N-1)]^{\mathrm{T}}$. At the ith iteration, only one component of $\boldsymbol{s}$ is updated, namely, $s(n)$ with $n = i \bmod N + 1$. Hence, the complement set is the vector $\boldsymbol{s}_{\overline{n}}$ obtained by omitting the component $s(n)$ in $\boldsymbol{s}$. From (12), $\boldsymbol{Y}$ can be expressed as

$$\boldsymbol{Y} = \boldsymbol{u}_n + \sum_{m=0, m \neq n}^{N-1} \boldsymbol{h}_m s(m) \quad (13)$$

where

$$\boldsymbol{u}_n = \boldsymbol{h}_n s(n) + \boldsymbol{W}, \quad n = 0, 1, \dots, N-1 \quad (14)$$

We choose $\boldsymbol{u}_n$, $n = 0, 1, \dots, N-1$ as hidden data when estimating $s(n)$. Let the conditional log-likelihood function for the hidden data $\boldsymbol{u}_n$ be denoted by $\ell(\boldsymbol{u}_n|s(n)) \triangleq \log p(\boldsymbol{u}_n|s(n))$. At the ith iteration step, the expectation step (E-Step) of the SAGE algorithm computes the $Q(\cdot|\cdot)$ function as

$$Q_n(s(n)|\boldsymbol{s}^{(i)}) = E\{\ell(\boldsymbol{u}_n|s(n), \boldsymbol{s}_{\overline{n}}^{(i)})|\boldsymbol{Y}, \boldsymbol{s}^{(i)}\} \quad (15)$$

In the maximisation step (M-Step), only $s(n)$ is updated, that is

$$s^{(i+1)}(n) = \arg\max_{s(n)} Q_n(s(n)|\boldsymbol{s}^{(i)})$$
$$\boldsymbol{s}_{\overline{n}}^{(i+1)} = \boldsymbol{s}_{\overline{n}}^{(i)} \quad (16)$$

4.1 E-Step

From (14), $\ell(\boldsymbol{u}_n|s(n))$ can be expressed as

$$\ell(\boldsymbol{u}_n|s(n)) \propto \Re\{s^*(n)\boldsymbol{h}_n^{\dagger}\boldsymbol{u}_n\} - \frac{1}{2}|s(n)|^2\|\boldsymbol{h}_n\|^2 \quad (17)$$

Substituting (17) into (15), the E-Step yields

$$Q_n(s(n)|\boldsymbol{s}^{(i)}) = E\{\Re\{s^*(n)\boldsymbol{h}_n^{\dagger}\boldsymbol{u}_n^{(i)}\} - \frac{1}{2}|s(n)|^2\|\boldsymbol{h}_n\|^2\} \quad (18)$$

where

$$\boldsymbol{u}_n^{(i)} \triangleq E\{\boldsymbol{u}_n|\boldsymbol{Y}, \boldsymbol{s}^{(i)}\}$$

The expectation should be taken with respect to the conditional distribution $p(\boldsymbol{u}_n|\boldsymbol{Y}, \boldsymbol{s}^{(i)})$. From (14) and the fact that $\boldsymbol{W} = \boldsymbol{Y} - \sum_{n=0}^{N-1} \boldsymbol{h}_n s(n)$, it follows easily that

$$\boldsymbol{u}_n^{(i)} = \boldsymbol{h}_n s^{(i)}(n) + \left(\boldsymbol{Y} - \sum_{m=0}^{N-1} \boldsymbol{h}_m s^{(i)}(m)\right) \quad (19)$$

4.2 M-Step

In the maximisation step, each component of $\boldsymbol{s}^{(i+1)}$ can be obtained by maximising the right-hand side of (18), i.e.

$$s^{(i+1)}(n) = \arg\max_{s(n)} \{\Re\{s^*(n)\boldsymbol{h}_n^{\dagger}\boldsymbol{u}_n^{(i)}\} - \frac{1}{2}|s(n)|^2\|\boldsymbol{h}_n\|^2\} \quad (20)$$

for $n = 0, 1, \dots, N-1$.

We can summarise now the SAGE algorithm as follows:

- For $i = 0$, determine the initial value of $\boldsymbol{s}^{(i)}$, namely, $\boldsymbol{s}^{(0)} = [s^{(0)}(0), s^{(0)}(1), \dots, s^{(0)}(N-1)]^{\mathrm{T}}$.

- At the $(i+1)$th iteration $(i = 0, 1, 2, \dots)$: for $n = (i+1) \bmod N + 1$, compute $s^{(i+1)}(n)$ from (20).

Note that, for constant envelope modulation, the term $\|\boldsymbol{b}_i\|^2$ can be removed from the maximisation process. In this case

$$s^{(i+1)}(n) = \arg\max_{s(n)}\{\Re\{s^*(n)\boldsymbol{b}_n^\dagger \boldsymbol{u}_n^{(i)}\}\}, \quad n = 0, 1, \ldots, N-1$$

(21)

4.3 Initialisation

Although the convergence of the SAGE and EM algorithms to global extremum points has not been proven for the detection problem where the parameter set is discrete, in practice, these algorithms do converge if initialised properly. Therefore the initialisation step is crucial for this problem. In this work, initialisation has been achieved by means of a low-complexity linear MMSE algorithm. It is known that the solution obtained by MMSE detection is a good candidate for the initial point. However, as noted previously MMSE detection has an error floor for high SNR values because of ICI. Thus, the SAGE algorithm with MMSE initialisation achieves the V-BLAST performance for lower SNR values while its performance degrades for higher SNR values.

From the observation equation (10), the initial value of data can be obtained by MMSE expressed as

$$\boldsymbol{s}^{(0)} \equiv \widehat{\boldsymbol{s}}_{\mathrm{MMSE}} = (\boldsymbol{H}^\dagger \boldsymbol{H} + \sigma_w^2 \boldsymbol{I}_N)^{-1}\boldsymbol{H}^\dagger \boldsymbol{Y} \qquad (22)$$

The matrix inversion in (22) requires $O(N^3)$ complex operations, which is computationally very intensive when N is large such as for the IEEE 802.11 and IEEE 802.16 families. However, time-varying channels produce a nearly banded channel matrix whose only main diagonal, Q subdiagonals and Q superdiagonals are non-zero. The bandwidth $2Q$ is a parameter to be adjusted according to the mobility rate of the channel and it has been determined that $Q = \lfloor f_d T \rfloor + 1$ is an appropriate choice for Rayleigh fading [15]. Therefore the banded property of $\boldsymbol{H}$ can be exploited to reduce the computational complexity by means of low-complexity decompositions such as the Cholesky or the $LL^\dagger$ factorisation of Hermitian banded matrices. Since $\boldsymbol{T} \triangleq \boldsymbol{H}^\dagger \boldsymbol{H} + \sigma_w^2 \boldsymbol{I}_N$ in (22) is a Hermitian banded matrix with lower and upper bandwidth $2Q$, we choose the $LL^\dagger$ factorisation to obtain $\boldsymbol{T}^{-1}$ which has the advantage of not requiring a square root. The basic steps of the data detection are given below [15]:

- Construct the banded matrix $\boldsymbol{T} = \boldsymbol{H}^\dagger \boldsymbol{H} + \sigma_w^2 \boldsymbol{I}_N$.

- Noting that $\boldsymbol{T}$ is a positive definite matrix, perform the $LL^\dagger$ Cholesky factorisation of $\boldsymbol{T}$, as expressed by $\boldsymbol{T} = \boldsymbol{LL}^\dagger$, where the triangular factor $\boldsymbol{L}$ has lower bandwidth $2Q$.

- Compute $\boldsymbol{r} = \boldsymbol{H}^\dagger \boldsymbol{Y}$ and solve the system $\boldsymbol{Td} = \boldsymbol{r}$ for $\boldsymbol{d}$ by the following steps:

(1) solve the triangular system $\boldsymbol{Lf} = \boldsymbol{r}$ for $\boldsymbol{f}$;

(2) solve the triangular system $\boldsymbol{L}^\dagger \boldsymbol{d} = \boldsymbol{f}$ for $\boldsymbol{d}$.

- Then $\widehat{\boldsymbol{s}}_{\mathrm{MMSE}} = \boldsymbol{d}$.

4.4 Complexity requirements

The computational complexity of the SAGE algorithm proposed in this work is determined by the parameters Q, N and the constellation type of the transmitted data symbols. Taking into account that $\boldsymbol{H}^\dagger \boldsymbol{H}$ is a nearly banded with bandwidth $4Q$, it was shown in [15] that computation of initial data symbols $\boldsymbol{s}^{(0)}$ require $(4Q^2 + 12Q + 2)N$ complex multiplications (CMs), $(4Q^2 + 8Q + 1)N$ complex additions (CAs) and $(2Q + 1)$ complex divisions leading to a total of $(8Q^2 + 22Q + 4)N \sim O(Q^2 N)$ complex operations. On the other hand, for iterations $i = 1, 2, \ldots$, the SAGE algorithm given in (20) can be expressed as

$$s^{(i+1)}(n) = \arg\max_{s(n)}\left\{\Re\left\{s^*(n)\left(\boldsymbol{b}_n^\dagger \boldsymbol{Y} - \sum_{m=0, m\neq n}^{N-1}\boldsymbol{b}_n^\dagger \boldsymbol{b}_m s^{(i)}(m)\right)\right. \right.$$
$$\left.\left. -\frac{1}{2}|s(n)|^2\|\boldsymbol{b}_n\|^2 \right\}\right\} \qquad (23)$$

The quantities $\boldsymbol{b}_n^\dagger \boldsymbol{b}_m$ and $\boldsymbol{b}_n^\dagger \boldsymbol{y}$ in (23) are calculated during the initialisation step, from $\boldsymbol{H}^\dagger \boldsymbol{H}$ and $\boldsymbol{H}^\dagger \boldsymbol{Y}$, respectively. Therefore they do not need to be calculated again. If we do not count the argmax operation that corresponds to the demodulation of the signal and assume that the SAGE algorithm converges in two stages ($2N$ iterations), the computation of (23) requires $2(4Q + 2)N$ CMs and $2(4Q + 2)N$ CAs, i.e., roughly $O(QN)$ complex operations for non-constant envelope signal constellations. Finally, sorting the OFDM subbands according to their estimated strengths require $N \log N$ complex operations. Consequently, the total computational complexity to implement our equalisation/detection algorithm is $O((Q^2 + \log N)N)$.

On the other hand, several low-complexity frequency-domain equalisation algorithms have been developed, recently, for OFDM receivers operating in the presence of high mobility, based on the banded property of the channel matrix [15–17]. Two of them are worth mentioning here to compare their computational complexities with that of our equalisation/detection algorithm. In these works, the problem of equalising an OFDM signal subject to channel variations is achieved in the frequency domain and the authors focus on the complexity reduction of the matrix inversion for the MMSE detection. Ruguni *et al.* [15] proposed block MMSE equalisation based on exploiting the banded structure of the channel matrix. The matrix inversion was obtained using one of the low-complexity decomposition techniques. The algorithm requires a total of $(8Q^2 + 22Q + 4)N \sim O(Q^2 N)$ complex operations.

Schniter [16] proposed a linear serial equaliser also based on exploiting the banded structure of the channel matrix and on splitting the channel matrix into several smaller size submatrices from which soft data are detected serially. This algorithm requires a total of $(8/3Q^3 + 2Q^2 + 5/3Q + 4)$ $N \sim O(Q^3 N)$ complex operations. The complexity of the serial MMSE equaliser is higher than that of the block MMSE equaliser. Another similar technique for linear MMSE equalisation that decomposes the channel matrix into several small sub-matrices and then applies a successive interference cancellation method was proposed in [17]. However, it was shown that its performance is well below that of the VBLAST algorithm.

VBLAST, another equalisation/detection algorithm, yields substantially better error performance than conventional linear equaliser/detectors. As explained in Section 2, the algorithm performs four steps: nulling, slicing, cancelling and ordering. Estimation of the symbols is done at the slicing stage and a new received signal is calculated by subtracting the estimated symbols. If we do not count the slicing operation that corresponds to the demodulation, the nulling and cancelling processes require $2N$ CMs and $2N - 1$ CAs for each iteration leading to a total of $(4N - 1)N \sim O(N^2)$ complex operations. Also, ordering of the symbols requires an $N \times N$ matrix inversion and sorting in each iteration loop. The repeated inverse matrix computation in the ordering step is the main computational bottleneck of the algorithm and it requires total a total of a $O(N^4)$ complex operations for detection of all the N data symbols. However by using the banded structure of the channel matrix this complexity can be reduced to $O(Q^2 N^2)$ using Rugini's approach [15]. In addition to this, as can be seen from Table 2, computation of the signal-to-interference plus noise ratio (SINR_k) in each iteration step k requires $N^2 + 2N + 2$ CMs and N^2 CAs, leading to a total of $O(N^3)$ complex operations. As a result, the whole VBLAST algorithm needs approximately $O(N^3) + O(N^2 Q^2) + O(N^2)$ complex operations. Therefore the computational complexity of the VBLAST receiver increases rapidly with the number of subcarriers which makes its real-time implementation prohibitive for OFDM-based WiMAX and LTE types of systems.

Based on the above discussions on computational complexities of different equalisation algorithms, we conclude that the complexity of our algorithm has the same order as that of the serial and block equalisation algorithms and is much lower than that of the VBLAST algorithm. However, as remarked earlier, linear equalisation/detection algorithms are suboptimal and perform poorly especially when the ICI is high. This fact can be seen clearly in the computer simulation results presented in the next subsection. On the other hand, our algorithm achieves the VBLAST performance for lower SNR values. Its performance degrades a bit at higher SNR values mainly because the MMSE algorithm adopted for initialisation of the SAGE algorithm exhibits an error floor at high SNR

values. This problem might be avoided by choosing a better initialisation algorithm.

5 Simulation results

In this section, the SER performance of the OFDM receivers described above operating over fast-frequency-selective channels is investigated using computer simulations. There are two existing strategies for ranking the subbands for SAGE receivers. The first one is that the subbands are sorted according to their estimated strength, so that the subband with the weakest strength is ranked first. The other one is that the subbands are ranked in order of decreasing strength. Note that in [10], the first sorting method yields better performance. Therefore the first sorting method is used for all SAGE simulations. In these simulations, perfect knowledge of the channel transfer function at the receiver is assumed. For the simulations, to demonstrate the exact performance of the investigated and proposed receivers the full channel matrix is considered ($Q = N$). We investigate here four scenarios to asses performance of the detection algorithms because WiMAX/LTE like systems support different modulation types to optimise the performance of the system under various propagation conditions. The simulation parameters of the first scenario are comparable to those used in [6].

5.1 Scenario-1

The system operates with a 1 MHz bandwidth and is divided into 32 tones ($N = 32$) with a total symbol period of 40 μs, of which 8 μs constitutes the CP. One OFDM symbol thus consists of 40 samples ($N + G = 40$), eight of which constitute the CP. We assume that the root-mean square (rms) width of the channel power-delay profile is $\tau_{\mathrm{rms}} = 1$ sample (1 μs) [18].

In Figs. 1 and 2, the SERs of binary PSK (BPSK) and quadrature PSK (QPSK) are shown as functions of SNR when the normalised Doppler frequency $f_d T = 0.05$. Results are shown for MF, ZF, MMSE, VBLAST and SAGE receivers. As expected, it is seen that MMSE detection outperforms MF and ZF detection. It is also seen that the MF suffers from severe ICI whereas ZF detection has a smaller error floor than the MF. The SAGE algorithm has comparable performance with VBLAST. In particular, it is seen that the SAGE algorithm exhibits a detection gain of about 1.5 and 3.5 dB over MMSE detection for BPSK and QPSK modulations at $\mathrm{SER} = 10^{-3}$, respectively. Moreover, it is also seen that the detection gain of SAGE over MMSE increases for higher SNR values. The reason the SAGE performance is sightly lower than that of VBLAST for higher normalised Doppler frequency is that the initialisation of the SAGE experiences ICI or noise enhancement.

Fig. 3 illustrates the behaviour of the SER against the number of iterations for the SAGE algorithm. It is seen
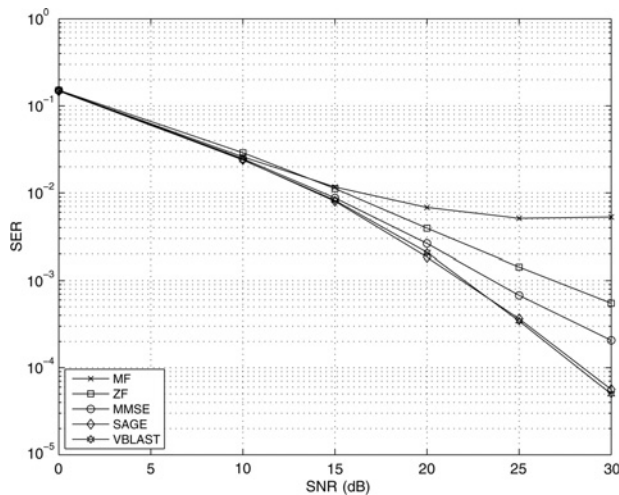
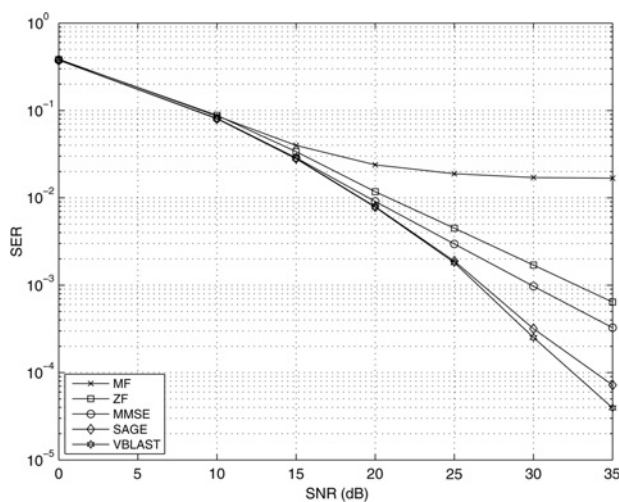**Figure 1** *Performance comparisons of detection algorithms (BPSK, fdT = 0.05)*

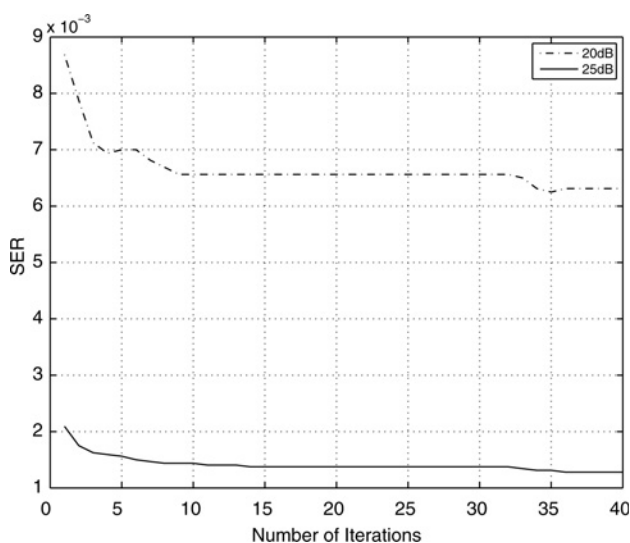**Figure 2** *Performance comparisons of detection algorithms (QPSK, fdT = 0.05)*

Figure 3 *Behaviour of the SER with respect to the number of iterations for the SAGE algorithm (QPSK, fdT = 0.1)*

that the SAGE algorithm converges within 35 iterations in this case. Since all the data are updated every N iterations, we count N iterations of the SAGE algorithm as one stage. In this sense, it can be also said that the SAGE algorithm converges within two stages.

5.2 Application Scenario-2

Although the scenario above is useful for comparing the VBLAST and SAGE algorithms, its parameters do not match mobile-WiMAX parameters as described in [19]. One of the most important parameters is the FFT size of the OFDM system. The number of subcarriers in the specified bandwidth is determined by the FFT size. Larger FFT sizes form narrower subcarriers and smaller inter-subcarrier spacing for fixed bandwidth. Narrower subcarriers lead to longer symbol times and to less susceptibility to delay spread but greater susceptibility to ICI, particularly for large Doppler. In mobile WiMAX, the FFT size is scalable from 128 to 2048. To maintain the OFDM symbol duration (also fixed subcarrier spacing) the available bandwidth increases when the FFT size is increased.

In our WiMAX application scenario, the system operates with a 5 MHz bandwidth and is divided into 512 tones ($N = 512$) with a total symbol period (T_s) of 115.2 μs, of which 12.8 μs constitute the CP. The sampling frequency is 5 MHz (i.e., the sampling time is equal to 200 ns). Therefore the subcarrier spacing of 9.76 kHz is chosen to satisfy the delay spread and Doppler spread requirements for mobile environments. One OFDM symbol thus consists of 576 samples, 64 of which constitute the CP. The normalised Doppler frequencies are $f_{d1}T = 0.0307$ and $f_{d2}T = 0.0614$, corresponding to an IEEE 802.16e mobile terminal moving with speeds v of 120 and 240 km/h, respectively, for a carrier frequency of 2.4 GHz.
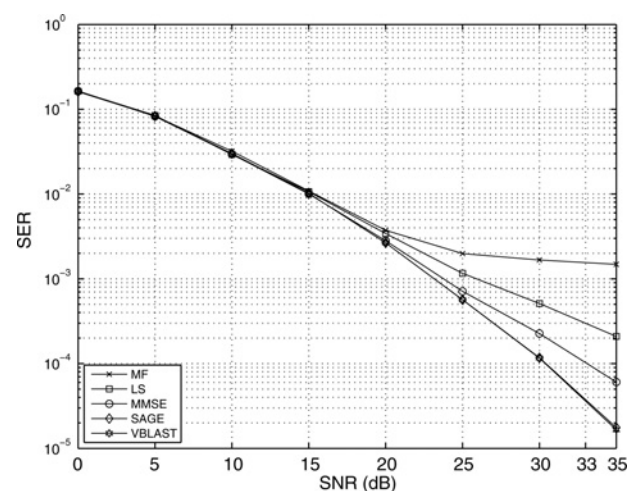

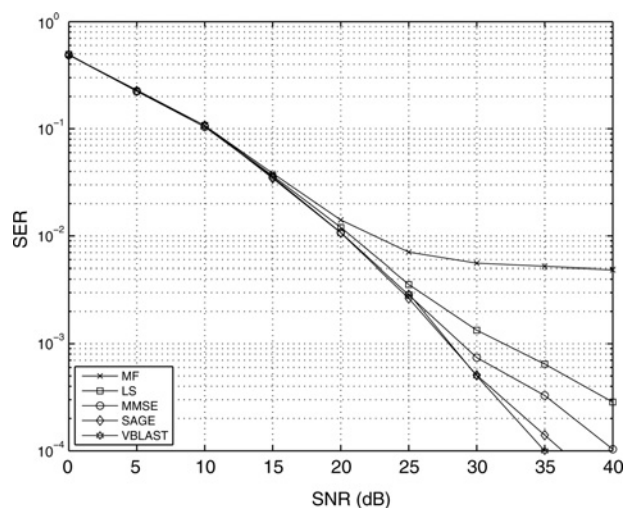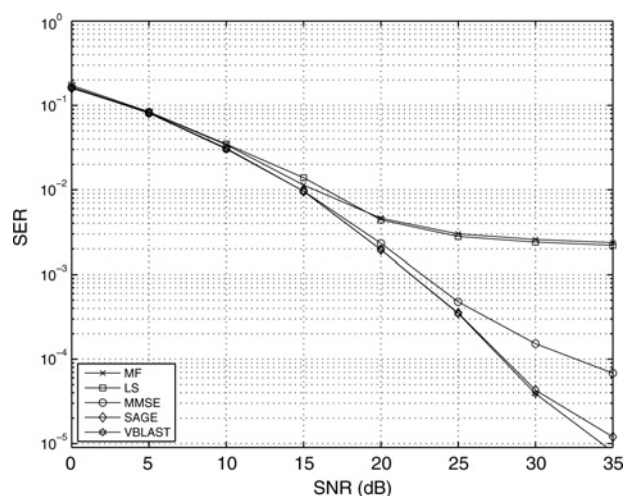**Figure 4** *Performance comparison of detection algorithms (BPSK, v = 120 km/h)*

Figure 5 *Performance comparison of detection algorithms (QPSK, v = 120 km/h)*

Figure 7 *Performance comparison of detection algorithms (QPSK, v = 240 km/h)*

In Figs. 4 and 5, the SERs of BPSK and QPSK are shown as functions of SNR for a speed of 120 km/h. It is observed that SAGE outperforms ZF, ML and MMSE receivers while it has similar performance to VBLAST. In particular, it is observed that savings of about 3 dB is obtained at $SER = 10^{-4}$, as compared with the MMSE detection for BPSK and QPSK modulations. It is concluded that initialisation of the SAGE algorithm is satisfactory for the speed of 120 km/h.

In Figs. 6 and 7, the speed of the mobile terminal is increased to 240 km/h for both BPSK and QPSK. In this case, it is seen that the SERs of the linear equalisers increase because of ICI or noise enhancement. In particular, performance of LS degrades especially for BPSK signalling and higher Doppler frequencies. On the other hand, it is also observed that the performance difference between the MF and LS increases for higher modulation

types. It is concluded that the MF and LS receivers fall short of expectations for the WiMAX standard. Moreover, it is seen that the performance of the VBLAST and SAGE algorithms is improved because of the time diversity [6]. Therefore the SNR gain of the SAGE algorithm is increased significantly relative to MMSE detection for both BPSK and QPSK modulations. For example, it is seen that a savings of about 5 dB is obtained at $SER = 10^{-4}$, as compared with MMSE detection for BPSK. The performance improvement of the SAGE receiver in the case of high mobility thus indicates that it is a better choice for the WiMAX standard.

5.3 Application Scenario-3

The physical layer of WiMAX is quite flexible. Therefore data rate performance varies depending on the channel bandwidth, modulation and coding schemes used. In the downlink, 16QAM and 64QAM are mandatory for both fixed and mobile WiMAX; 64QAM is optional in the uplink. In this application scenario, we investigate the SER performance for 16QAM (4 bit/s/Hz) and 64QAM (6 bit/s/Hz) signalling constellations.

In Figs. 8 and 9, the SER performance of 16QAM and 64QAM is investigated for the speed of 120 km/h. It is seen that the MF receiver cannot be used for 16QAM signalling because it does not correct the envelope of the received signal. Moreover, it is shown that savings of about 7 dB are obtained at $SER = 10^{-4}$, as compared with MMSE detection for 16QAM and 64QAM.

In Figs. 10 and 11, it is demonstrated that the time diversity gain cannot be achieved for high mobility because the SER performance of the MMSE equaliser used for the initialisation is degraded significantly. In other words, the performance degradation for the linear equalisers is more obvious for higher-order modulations.
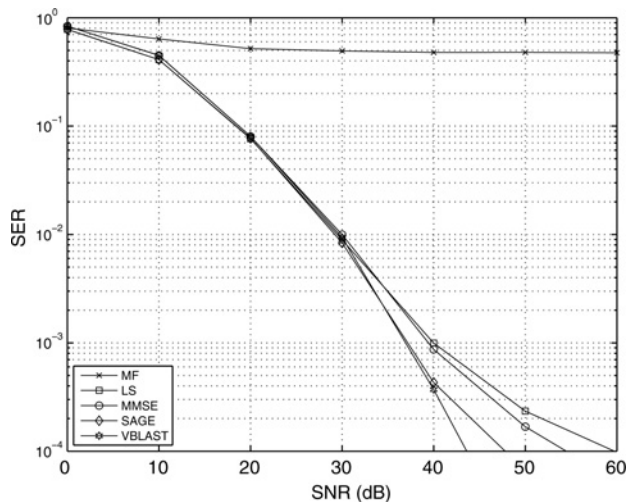

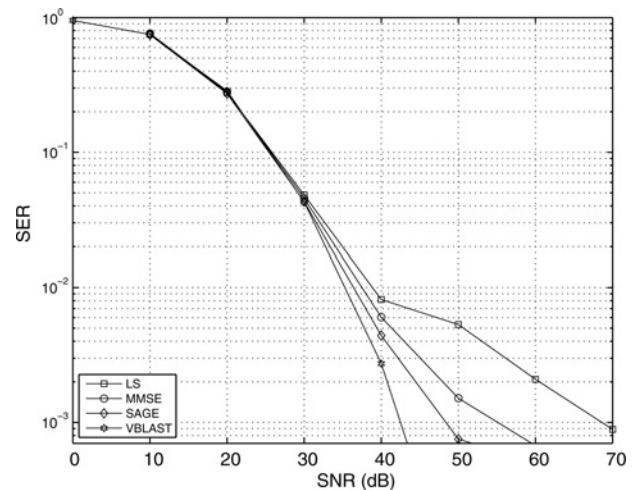**Figure 6** *Performance comparison of detection algorithms (BPSK, v = 240 km/h)*

Figure 8 *Performance comparison of detection algorithms (16QAM, v = 120 km/h)*

Figure 9 *Performance comparison of detection algorithms (64QAM, v = 120 km/h)*

Figure 10 *Performance comparison of detection algorithms (16QAM, v = 240 km/h)*

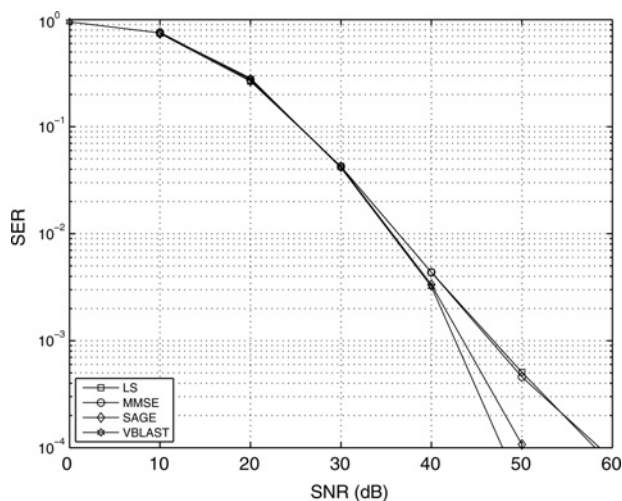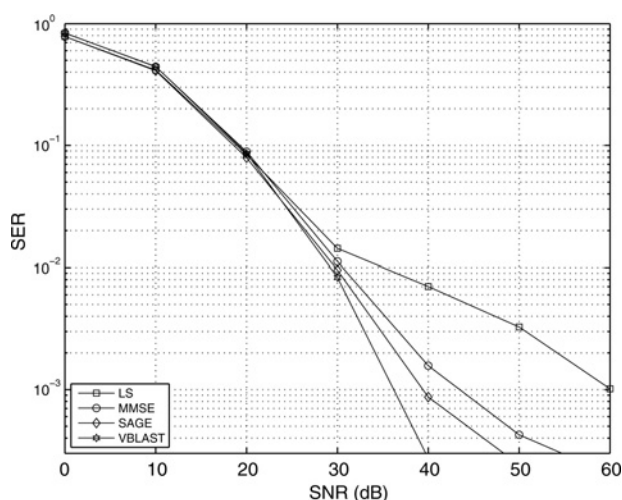**Figure 11** *Performance comparison of detection algorithms (64QAM, v = 240 km/h)*

Therefore the SAGE performance is also degraded. Yet, SAGE detection still outperforms MMSE detection significantly at $SER = 10^{-3}$. It is concluded that VBLAST outperforms the SAGE algorithm especially for higher modulation types, very high mobility and for high SNRs. On the other hand, as is explained in the complexity section, the complexity of VBLAST is significantly greater than that of SAGE algorithm. Thus, there is a clear tradeoff between these two.

5.4 Application Scenario-4

Bit error rate (BER) requirements for BWA operating environments according to quality of service classes are 10^{-3} to 10^{-7} for real time (constant delay) applications and are 10^{-5} to 10^{-8} for nonreal time (variable delay) applications [20, 21]. The performance of uncoded-OFDM over fading channels can be improved by introducing forward error correction coding. Therefore coding is an inseparable part of most OFDM applications. In this section, we investigate the BER performance of the proposed detection methods for coded OFDM systems.

In this application scenario, the BER performance of a 64QAM modulated coded-OFDM system is tested. The coding scheme we chose for our system is the $(13_8, 15_8)$ convolutional code with rate 1/2. Since burst errors deteriorate the performance of the coding scheme, the output sequence from the encoder is interleaved with a 48×64 block interleaver to spread the consequences of a local notch in the transfer function over the code sequence. In Fig. 12 the coded BER performance of the 64QAM modulated OFDM system is shown when the mobile terminal moves at a speed of 240 km/h. It is seen that the superiority of the SAGE algorithm holds also for coded-OFDM systems. Thus, coded-OFDM systems with SAGE detection can meet the expectations of next-generation wireless communications systems.
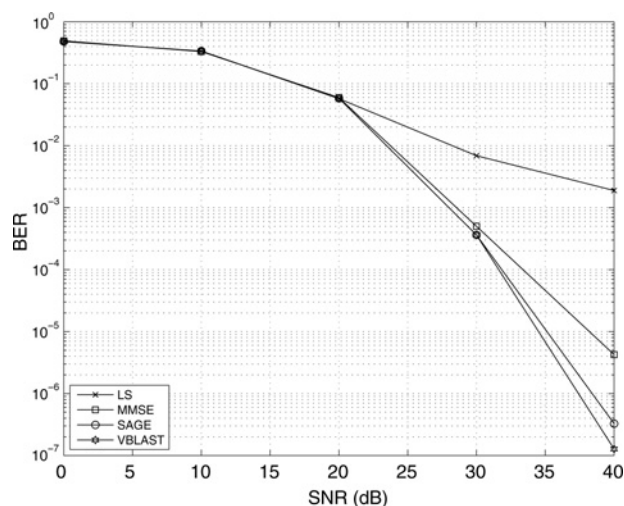
Figure 12 *Performance comparison of detection algorithms for coded-OFDM systems (64QAM, v = 240 km/h)*

6 Conclusion

In this paper, a SAGE-based low-complexity data detection and channel equalisation algorithm has been proposed. It has been observed that the algorithm updates the data sequences in series leading to a receiver structure that also incorporates ICI cancellation, enabling the system to operate at high vehicle speeds. Simulation results have confirmed that the proposed algorithm has lower SER than ZF and MMSE detection techniques in a variety of usage scenarios. Moreover, it has been shown that the SAGE detection technique has comparable performance to VBLAST while requiring significantly lower computational complexity. The computer simulations have demonstrated that the algorithm can be successfully employed in LTE and WiMAX systems with a capability of full mobility support.

7 Acknowledgments

8 References

[1] NI Q., VINEL A., XIAO Y., TURLIKOV A., JIANG T.: 'Investigation of bandwidth request mechanisms under point-to-multipoint mode of WiMAX networks', *IEEE Commun. Mag.*, 2007, **45**, (5), pp. 132–138

[2] EKLUND C., MARKS R., STANWOOD K., WANG S.: 'IEEE standard 802.16: a technical overview of the WirelessMAN TM air interface for broadband wirelessaccess', *IEEE Commun. Mag.*, 2002, **40**, (6), pp. 98–107

[3] DOGAN H., CIRPAN H.A., PANAYIRCI E.: 'Iterative channel estimation and decoding of turbo coded SFBC-OFDM systems', *IEEE Trans. Wirel. Commun.*, 2007, **6**, (8), pp. 3090–3101

[4] ZHANG J., MU X., CHEN E., YANG S.: 'Decision-directed channel estimation based on iterative linear minimum mean square error for orthogonal frequency division multiplexing systems', *IET Commun.*, 2009, **3**, (7), pp. 1136–1143

[5] KANG Y., KIM K., PARK H.: 'Efficient DFT-based channel estimation for OFDM systems on multipath channels', *IET Commun.*, 2007, **1**, (2), pp. 197–202

[6] CHOI Y.S., VOLTZ P.J., CASSARA F.A.: 'On channel estimation and detection for multicarrier signals infast and selective rayleigh fading channels', *IEEE Trans. Commun.*, 2001, **49**, (8), pp. 1375–1387

[7] POOR H.V.: 'Iterative multiuser detection', *IEEE Signal Process. Mag.*, 2004, **21**, (1), pp. 81–88

[8] NELSON L., POOR H.V.: 'Iterative multiuser receivers for CDMA channels: an EM-based approach', *IEEE Trans. Commun.*, 1996, **44**, (12), pp. 1700–1710

[9] DAI H., POOR H.V.: 'Iterative space–time processing for multiuser detection in multipath CDMA channels', *IEEE Trans. Commun.*, 2002, **50**, (9), pp. 2116–2127

[10] KOCIAN A., FLEURY B.: 'EM-based joint data detection and channel estimation of DS-CDMA signals', *IEEE Trans. Commun.*, 2003, **51**, (10), pp. 1709–1720

[11] DOGAN H.: 'EM/SAGE based ML channel estimation for uplink DS-CDMA systems over time-varying fading channels', *IEEE Commun. Lett.*, 2008, **12**, (10), pp. 740–742

[12] XIE Y., LI Q., GEORGHIADES C.N.: 'On some near optimal low complexity detectors for MIMO fading channels', *IEEE Trans. Wirel. Commun.*, 2007, **6**, (4), pp. 1182–1186

[13] JAKES W., COX D.: 'Microwave mobile communications' (Wiley-IEEE Press, New York, 1994)

[14] FESSLER J., HERO A.: 'Space-alternating generalized expectation-maximization algorithm', *IEEE Trans. Signal Process.*, 1994, **42**, (10), pp. 2664–2677

[15] RUGINI L., BANELLI P., LEUS G.: 'Simple equalization of time-varying channels for OFDM', *IEEE Commun. Lett.*, 2005, **9**, (7), pp. 619–621

[16] SCHNITER P.: 'Low-complexity equalization of OFDM in doubly selective channels', *IEEE Trans. Signal Process.*, 2004, **52**, (4), pp. 1002–1011

[17] KIM K., PARK H.: 'A low complexity ICI cancellation method for high mobility OFDM systems'. Proc. IEEE 63rd Vehicular Technology Conf., 2006, VTC 2006, Spring, Melbourne, Australia, 2006, vol. 5, pp. 2528–2532

[18] EDFORS O., SANDELL M., VAN DE BEEK J., WILSON S., BORJESSON P.: 'OFDM channel estimation by singular value decomposition', *IEEE Trans. Commun.*, 1998, **46**, (7), pp. 931–939

[19] YAGHOOBI H.: 'Scalable OFDMA physical layer in IEEE 802.16 WirelessMAN', *Intel Technol. J.*, 2004, **8**, (3), pp. 201–212

[20] 'IEEE 802.16sc-99/28, quality of service (QoS) classes for BWA' (IEEE 802.16 Broadband Wireless Access Working Group, 1999)

[21] TEE L.: 'Packet error rate and latency requirements for a mobile wireless access system in an IP network'. IEEE Vehicular Technology Conf., 2007, VTC2007, Fall, Baltimore, MD, USA, 2007, pp. 249–253